DOI: https://doi.org/10.24425/amm.2025.153470

J. KRAWCZYK[1*], K. PAŃCIKIEWICZ[1], Ł. FROCISZ[1], H. DANIELEWSKI[2], P. FURMAŃCZYK[2]

LASER WELDING AND REMELTING OF DC05 LOW CARBON STEEL

Laser welded joint of ferritic low carbon steel DC05 was manufactured as Tailored Blank and examined by non-destructive visual testing and destructive testing by macro- and microscopic examination and hardness measurements. The tensile strength of the welded joint was 280 MPa and corresponds to the tensile strength of the base material. Microscopic observations of thinner plate revealed heat affected zone with coarse grain, in contrast to the thicker plate where coarse grain was not observed. Detailed analysis of laser remelted area on plates after various cold deformation (1%, 4.15% and 12.5%) reveals a significant influence of the plate state on the occurrence of grain growth. The increase in the width of the coarse-grained zone after 12.5% deformation increases by approximately 60% compared to the undeformed state, regardless of the travel speed.

Keywords: Laser welding; laser remelting; welded joint; grain growth; critical strain

1. Introduction

Laser technology has significantly contributed to the development of new methods of manufacturing, joining and improving the properties of the material [1-5]. The use of a concentrated beam of photons allows for very quickly and precise heating of the material. As the energy of the laser beam increases, it is possible to obtain full remelting of any range of engineering materials, regardless of their melting point.

Laser joining of engineering materials is an issue widely studied in the scientific literature. The problems of joining materials such as titanium, cobalt, nickel, magnesium, iron and aluminium alloys were analysed [6-11]. One of the most important aspects of laser processing is microstructural changes occurring in the beam interaction area and heat affected zone. The laser power, scanning speed and the area of focus of the laser beam have a key influence on the changes in the structure of the material [12]. An important aspect of the laser remelting process is the strong anisotropy of the material properties resulting from a significant temperature gradient in the beam interaction area. New grains crystallize in highly metastable conditions from the liquid phase, which results in significant fragmentation of the dendritic structure, which is a direct consequence of the sudden cooling of the material [12-17]. This also applies to the change in the size of the crystallites in the remelting area. The crystallites size after SLM (selective laser melting) is related to the speed of heat removal from the material. The subsequent interaction of the laser beam causes an increase in the size of the crystallite. Reheating of the previously re-melted area will result in the expansion of the existing crystallite areas by the diffusion mechanism [13]. The formation of new and the growth of existing dendritic areas during SLM is explained by the nucleation of a material with a similar crystal structure to the starting material. Heterogeneous nucleation on the already existing grains will reduce the energy needed for the development of the structure in the area of the weld, which favours the growth of crystallites with a short time of beam interaction [14]. Refinement of the joint structure is possible by adding additional particles to the material. It takes place by heterogeneous nucleation of new regions on the introduced particles [17-21]. The refinement of the crystal structure is also possible by using the oscillating interaction of the laser beam and thus introducing significant thermal stresses to the material [18]. The growth of new crystallites is related to the crystallographic orientation of the base material. The build-up and growth of the crystalline regions in the weld strongly depend on the specific crystallographic orientation observed during laser remelting of material [16,22-24].

However, not only the structure of the re-crystallizing layer after the laser remelting process will have a significant impact on the material properties. The areas near the fusion line are of great importance as they may affect product properties. A common phenomenon observed in these areas is transcrystalline cracks. The significant temperature gradient generated during the pro-

1 AGH UNIVERSITY OF KRAKOW, FACULTY OF METALS ENGINEERING AND INDUSTRIAL COMPUTER SCIENCE, AL. MICKIEWICZA 30, 30-059 KRAKÓW, POLAND
2 KIELCE UNIVERSITY OF TECHNOLOGY, FACULTY OF MECHATRONICS AND MECHANICAL ENGINEERING, 7 TYSIĄCLECIA PAŃSTWA POLSKIEGO AV., 25-314 KIELCE, POLAND

* Corresponding author: jkrawcz@agh.edu.pl

cess leads to the appearance of meaningful thermal stresses in the material. In extreme cases, the value of stresses will exceed the material's resistance to cracking. Besides, rapid heating to high temperature can cause grain boundaries liquation, leading to the destruction of the product or a significant decrease in its functional properties [25,26]. Fragmentation of grains not remelted during the joining process by stresses generated in HAZ (heat-affective zone) was observed. After the critical strain is exceeded, the dominant mechanism will be the nucleation of new grains in the heated area. However, with a significant overheating of the material and a high-temperature gradient between the melted areas and the base material, the nucleation process will be difficult, because the growth time will be shorter than the nucleation and growth. The dominant factor influencing the geometrical dimensions of the structure in HAZ will also be the mobility of the interface. Higher mobility of the interface will result in the formation of a coarser-grained structure in the heat-affected zone (CGHAZ) [27]. Phase transformation during the welding process will also affect the microstructure of the joint and HAZ. In the steels with micro-additives, degenerated upper bainite was observed in the heat-affected zone at the fusion line, transforming into granular bainite and a ferritic-pearlitic structure as it moved away from the fusion line. The fragmentation of the grains was observed in the area close to the base material [28]. In the dual-phase steel, which uses the possibility of changing the phase composition by heat treatment to improve their properties, the softening of the material in the heat-affected area was observed for laser welding. Local martensitic islands were tempered, reducing the functional properties of the element [29]. The grain fragmentation phenomenon was also observed in NPC steel. In the heat affected zone, areas with an enlarged grain, areas of fine grain and mixed grain are visible. Fragmentation is caused by heating the material to the temperature range close to the end of dissolution of the hypoeutectoid ferrite and martensitic transformation of supercooled austenite [30].

Laser welding is widely used in many industries, including in the automotive industry. Many different materials need to be welded [31]. Welded joints are made both between mild steel [32] and modern steels – Interstitial Free (IF) steels [33], High Strength Low Alloy (HSLA) steels [34,35], Advanced High-Strength Steels (AHSS) [36], Bake Hardening (BH) steels [37,38], Dual Phase (DP) steels [39-41], Transformation-Induced Plasticity (TRIP) steels [42], Complex-Phase (CP) steels [43], martensitic steels [44] and austenitic steels [45]. To reduce the weight of vehicles, semi-finished sheet of various grades and/or thicknesses are. Tailored Blanks are used as structural parts in the body-in-white of cars for improving crash performance. Typical applications are pillars (A and B) or the inner structure of car doors, where different strengths in different regions are required [46,47].

The work aimed to analyze the possibility of making a joint by laser beam welding and to show the mechanism of the structure formation in this welded joint. This goal was achieved by metallographic macro- and microscopic observations of welded joint and re-melts fusion in deformed plates by tensile test. So far, the reasons for the grain growth occurring in HAZ during tailored blanks laser welding of steels have not been fully explained. The present study aimed to clarify this phenomenon based on the theory of critical strain under the conditions of plastic deformation of the sheet during cutting and intense/dynamic heating during laser welding.

2. Materials and methods

The butt welded joint of EN 10130: DC05+ZE (1.0312+ZE; ASTM A 1008: EDDS) plate with different thickness (t_1 = 0.6 mm, t_2 = 1.2 mm) was welded by the 521 laser beam welding (LBW) process without a filler metal. Design of the welded joint are presented in Fig. 1a. This joint was a part of a right front door of a passenger car (Fig. 1b).

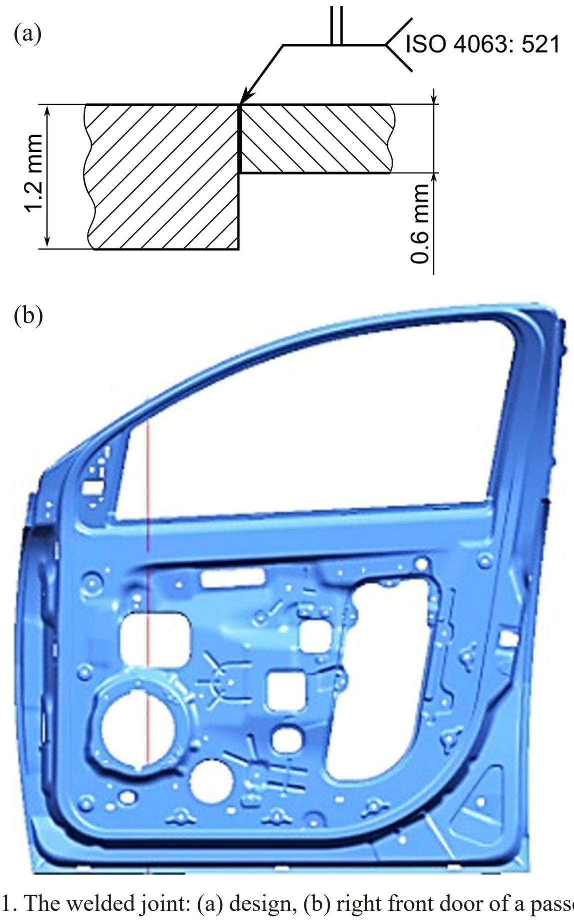

Fig. 1. The welded joint: (a) design, (b) right front door of a passenger car after welding and stamping. The place where the joint occurs is marked with a red line

To evaluate the influence of plastic deformation on the microstructure, annealed and cold deformed DC05+ZE plates with nominal thickness t_1 = 0.7 mm and t_2 = 1.2 mm was remelted by the 521 process, realized by Trumpf TLF 6000 Turbo. Process parameters are presented in TABLE 1. The travel speed and focus were variable for both plates thickness, remaining parameters were constant. Before the process, plates were soaked in a 40% hydrochloric acid solution to remove zinc coating. Appropriate degree of deformation was obtained by means static tensile tests, realized by Zwick/Roell Z250 with extensometer. The specimens was a flat with the dimension of L/W = 12.5/80 mm. The cleaned surface was covered by water glass before welding to improve the absorption.

Chemical composition of base metals was measured by Optical Emission Spectroscopy using a Foundry Master-WAS Spectrometer. Macro- and microscopic examinations were performed on cross sections after mechanical grinding, polishing and etching in 5% Nital reagent (5 ml HNO3 + 95 ml C2H5OH). Base metals, heat affected zones, weld metal and remelted areas were examined using light microscope Leica DM/LM. The grain size of base metals was quantified by the Jeffries method and the result was related to the grain size determined by ASTM E 112 [48]. Hardness measurements was performed by the Vickers method (2.96 N for HV0.3 and 4.93 N for HV0.5) with use Tukon 1202 universal hardness tester.

3. Results and discussion

Chemical compositions of base metals and mechanical properties, verified by the Optical Emission Spectroscopy and static tensile test, are presented in TABLE 2. Significant deviation between the inspection document and OES results in phosphorus content were found. The obtained value exceeds the content permitted by the EN 10130 [49] standard. In the case of manganese, the value is equal to the limit value. The results of the mechanical test showed that the strength and plastic properties are within the limits set by the EN 10130 [49] standard. Higher yield strength and lower elongation than the values from inspection documents may be due to the longer time between production and testing than the guaranteed 6 months and higher content of phosphorus. The long-term strain-ageing effect on the properties was observed on low-carbon steel reinforcement [50].

3.1. Welded joint analysis

The butt welded joint was B quality level (acc. to ISO 13919-1 [51]) in visual testing (VT) and macroscopic examination (Fig. 2). A weld was obtained with full penetration and a thickness not less than the joined thinner plate.

TABLE 1

Laser beam process parameters

Thickness, mm	Focus, mm	Travel speed m/min									
		0.50	0.57	0.65	0.75	0.86	1.00	1.31	1.50	1.72	2.00
0.7	60	—	—	—	x	x	x	x	x	x	x
	120	—	—	—	x	x	x	x	—	—	—
1.2	60	—	—	x	x	x	x	x	x	x	x
	120	x	x	x	x	x	—	—	—	—	—
Power: 1 kW; Frequency: 30 kHz; Beam diameter: 5 mm; Shielded gas: argon											

TABLE 2

Chemical composition and mechanical properties of base metals

Steel DC05	Chemical composition, mass %								Mechanical properties		
	C	Si	Mn	P	S	Al	Ti	Nb	R_e, MPa	R_m, MPa	A_{80}, %
EN 10130 standard [49]	≤ 0.06	—	≤ 0.35	≤ 0.025	≤ 0.025	—	—	—	≤ 180	270-330	40
Inspection documents	0.0011	0.02	0.12	0.006	—	0.036	0.028	0.014	155	294	45
OES/tensile tests results	0.02	0.08	0.35	0.042	0.006	0.029	0.029	0.023	160	280	41

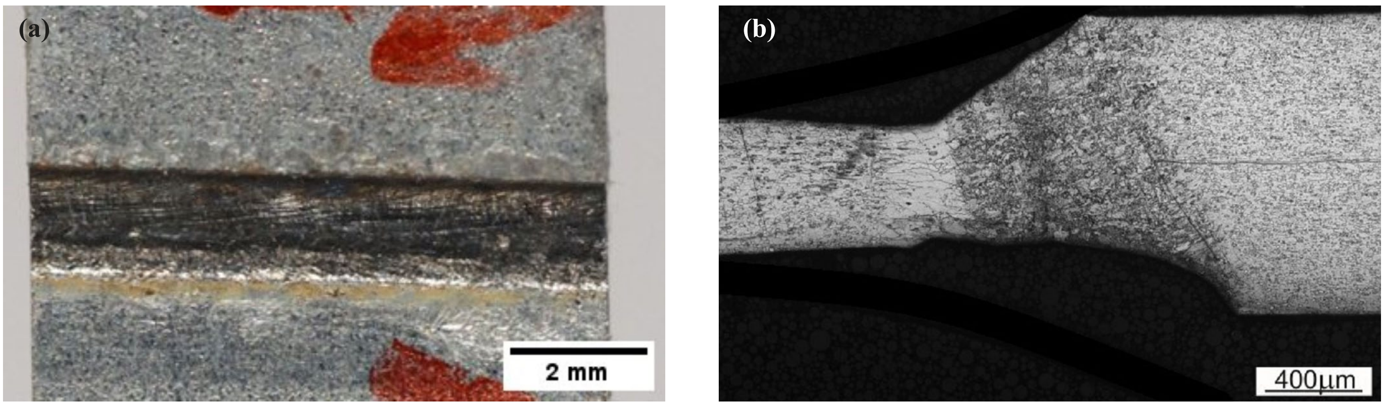

Fig. 2. General view (a) and macrostructure (b) of the welded joint. Regular shape of the weld with a smooth transition to the base material, without welding imperfections

Fig. 3 presents the microstructure of the welded joint. Base metals (Fig. 3a-b) was characterized by ferrite with equiaxial grain, which indicates a annealing delivery condition. The grain size was A = 143 μm^2, which corresponds to G = 10 acc. to ASTM E 112 [48]. In the heat affected zone of thinner plate (Fig. 3c) coarse and elongation grain in the area up to 300 μm from the fusion line were observed. Contrariwise, the growth of grain in the thicker plate is almost imperceptible (Fig. 3d).

In the heat-affected zone of laser-welded joints of steel with the BCC crystal lattice matrix, the most frequently observed coarse-grain zone (CGHAZ), fine-grain zone (FGHAZ) and the area of partial recrystallization (ICHAZ) of variable equiaxial grain size [52]. Mei et al. [53] observed conventional HAZ in DC03 and DC56D steels welded with CO_2 and fiber laser, and Zdravecká and Slota [54] in DX53D and DX54D steels welded with CO_2 laser. Danielewski and Skrzypczyk [55] observed conventional HAZ in S235JR steel steels welded with CO_2 laser. The research by Lisiecki et al. [56] and Prijanovič et al. [57] on DC04 and U/AHSS Docol® 1200M steels revealed the effect of reducing laser power on limiting grain growth in CGHAZ. This effect was observed in the work of Gonçalves et al. [58], Luo et al. [59] and Antunes and Lima [60] on AISI40, DC52D and DP600 steels. Contrariwise, in the laser welded joint of the DP-600MC and DC06EK steels, analyzed by Mihalikova et al. [61], elongated grain growth in CGHAZ is visible. Excessive grain-growth in HAZ during the welding of IF steels were observed by Bayraktar et al. [27,62] in welded joints made by Gas Tungsten Arc Welding (GTAW) and Resistance Spot Welding (RSW).

To explain the excessive grain growth, a thesis was put forward, according to which the grain growth in the HAZ is related to the recrystallization of the deformed material in the critical strain range, which is caused by a portion of heat input into the material during welding.

Hardness of the thinner plate was 152 HV0.3 and of the thicker plate was 145 HV0.3. The decrease in hardness is observed in the coarse grain HAZ of the thinner plate (140 HV0.3), while in the thicker one it increases (180 HV0.3). Hardness of the weld was 176-215 HV0.3. In the static tensile tests the material broke in the thinner base material with tensile strength *Rm* = 280 MPa. The values exceed the minimum requirements for the base material (TABLE 2) and correspond with base metal tensile strength, which is the expected effect.

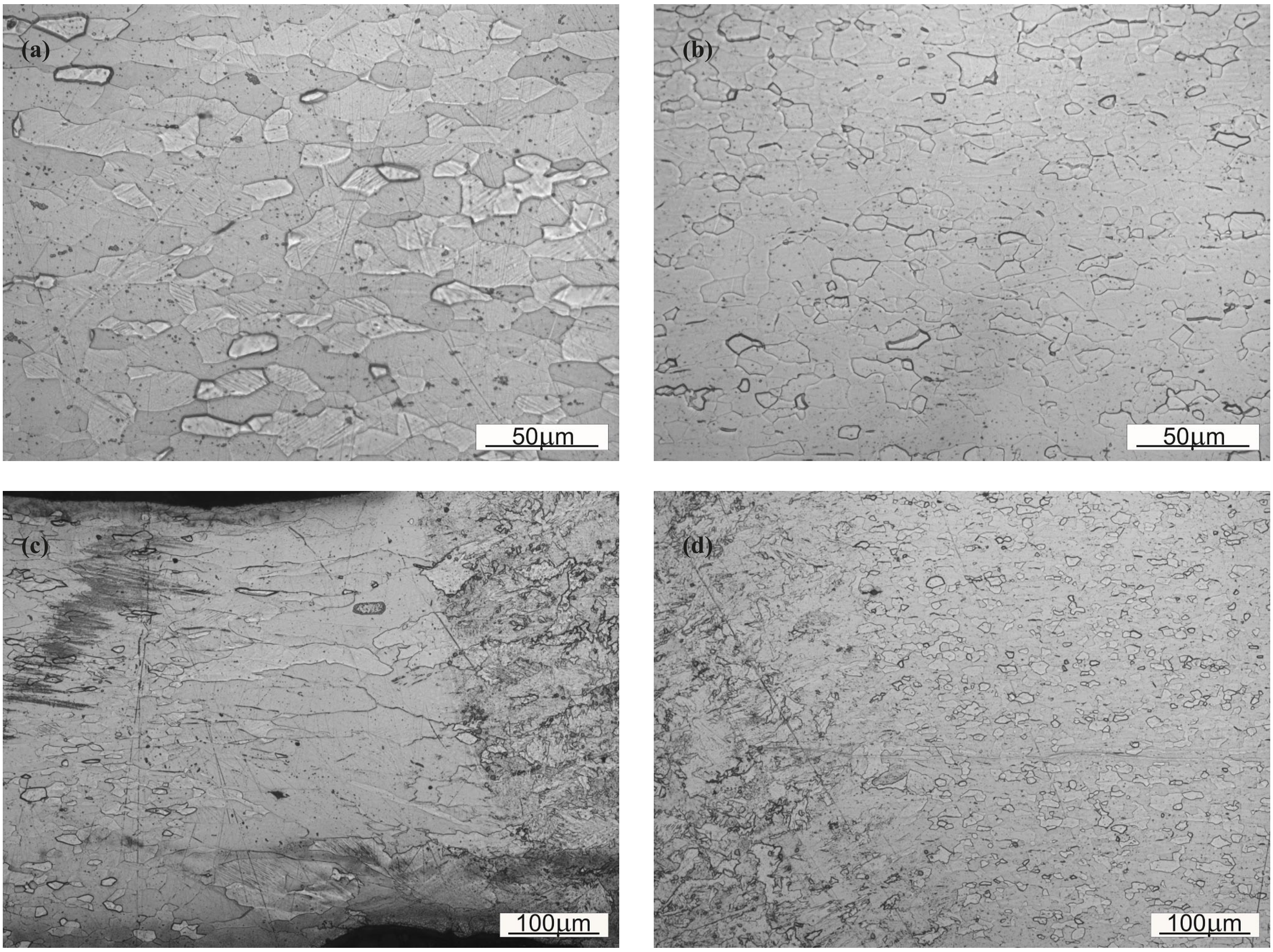

Fig. 3. Microstructure of DC05 steel: (a) base metal of thinner plate, (b) base metal of thicker plate, (c) heat affected zone in thinner plate, (d) heat affected zone in thicker plate (5% nital etched). Significant difference in the structure of the HAZ despite the similar input microstructure of both plates

3.2. Influence of laser beam parameters on the shape of structure transformation area

In order to confirm the thesis, the parameters of the laser remelting process were selected. The process and measurement scheme is shown in Fig. 4a. Fig. 4b presents the influence of laser beam remelting parameters on the width and height of structure transformation area (remelted area with heat affected zone). The width and depth of this area decrease with increasing travel speed and focus, which is the expected effect, observed e.g. by Lisiecki et al. [56] and Prijanovič et al. [57]. Doubling the focus causes a decrease in the remelting width by 17-25% in the top of the remelting and by 30-47% in the centre and at the bottom of the remelting. Increasing the thickness from 0.7 mm to 1.2 mm with a focus of 60 mm reduces the penetration width in the top by 38-53%. For both plates, at travel speeds higher than 1000 mm/min and focus of 60 mm, the penetration depth tends to 0. In any case, the smallest fusion width occurs in the middle of the plate thickness, which is related to the greatest number of heat discharge directions. This profile is often observed in laser beam welded joints [43,63-65]. To investigate influence of deformation on the grain size after remelting with a laser beam, the parameters including the focus of 60 mm and the travel speeds of 860 and 750 mm/min were selected.

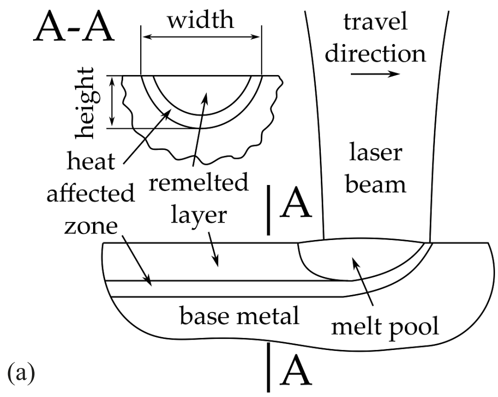

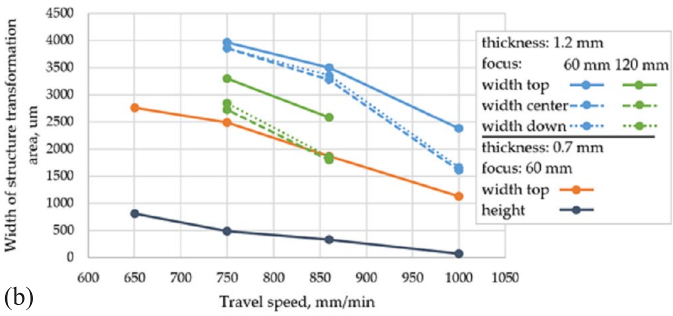

Fig. 4. (a) Schematic of laser beam remelting, (b) Influence of travel speed and focus on the width and height of structure transformation area

3.3. Influence of deformation on the grain size after laser beam remelting

On the basis of the stress-strain diagram (Fig. 5a), three ranges of sample deformation were selected: 1%, 4.15% and 12.5% of elongation. The samples deformed in a controlled manner were remelted with laser beam in the same way as in Fig. 4a. Regardless of the travel speed of the laser beam, the remelted layer width and the heat-affected zone increases with the increase of deformation (Fig. 5b). The change in the depth of remelting observed in the diagram is results from the change in the cross-section of the sample after its plastic deformation and in fact in all cases was 100% of the plate thickness.

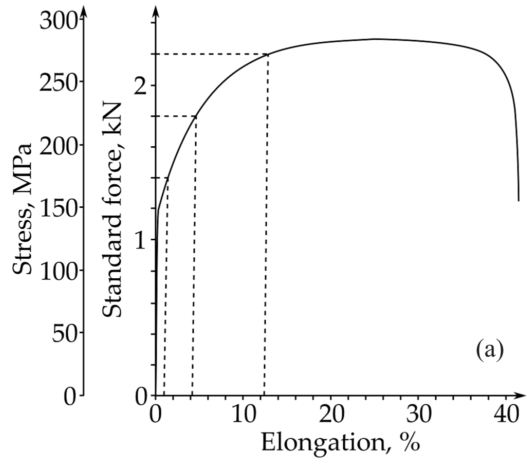

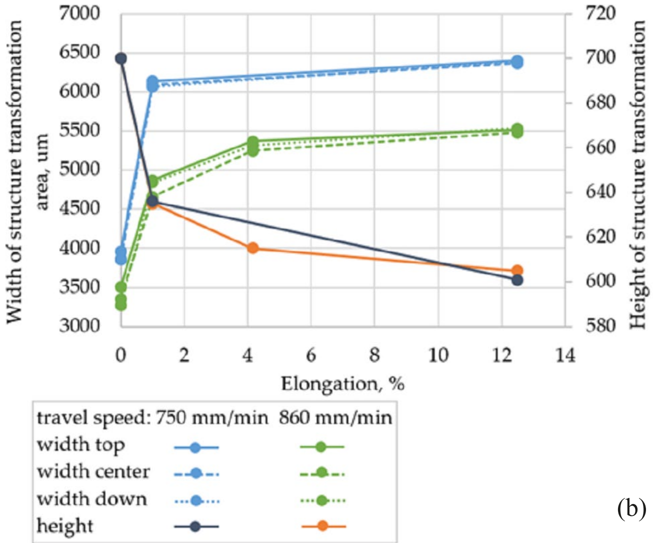

Fig. 5. (a) Stress-strain diagram, (b) influence of elongation on the width and height of structure transformation area

Detailed analysis of the microstructure of the analyzed samples showed that the width of the area of the coarse grain heat affected zone increased with the increase of the travel speed of the laser beam. In the non-deformed plate, near the fusion line, coarse grain area was not observed (Fig. 6a), similar to the Gonçalves et al. [58], Luo et al. [59] and Antunes and Lima [60] research. As the deformation of the sheets increased, the width of the CGHAZ increased (Fig. 6b-d) and the grain shape differed from equiaxial to elongated in the direction of heat flow. Moreover, CGHAZ hardness increased from 70 HV0.5 to 85 HV0.5 with the increase of deformation before remelting. The above experiment proves that in the case of cold rolled low carbon steels, the influence of deformation on grain growth is crucial.

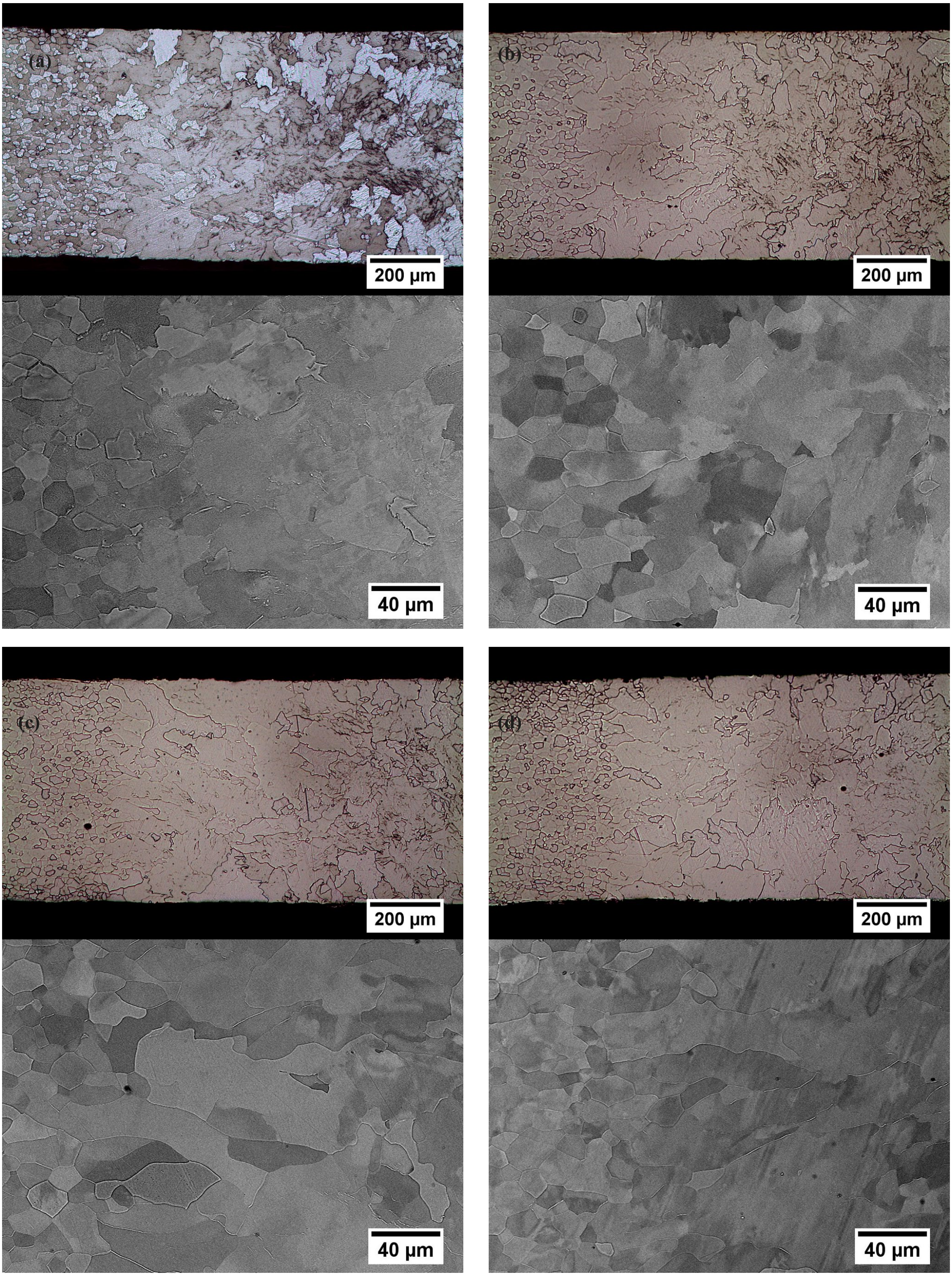

Fig. 6. Microstructure of remelted area with travel speed of 860 mm/min and heat affected zone of DC05 steel: (a) non-deformed plate, (b) deformed plate with 1% of elongation, (c) deformed plate with 4.15% of elongation, (d) deformed plate with 12.5% of elongation

4. Conclusions

1. The grain size in CGHAZ is strongly dependent on the degree of cold deformation. As the deformation increases, the width of the CGHAZ and the grain size increases. Thus, it is possible to control grain size in the laser remelting process through thermo-mechanical processes preceding remelting. A deformation degree of 12.5% increases the width of the CGHAZ by approximately 60%.
2. As the travel speed of the laser beam and the focus increases, the width and depth of the remelting area and HAZ are reduced. The reduction in the remelting width is from 11 to 24% and the remelting depth is approximately 32% for each increase in the travel speed by 100 mm/min.
3. To avoid unfavorable grain growth in CGHAZ, cold shaping of the plates before welding should be avoided. Preparing the edges of the elements for welding should be performed in a way that does not introduce significant deformation in the area of the cut.

Funding

This research was supported by the Polish Ministry of Science and Higher Education (Poland), grant number 16.16.110.663 (in AGH University of Science and Technology).

Acknowledgments

The authors are grateful to Łukasz Cabała, Kamila Kowalik and Jagoda Kaptur for the sample preparation and analysis.

REFERENCES

[1] Q. An, D. Wu, P. Liu, Y. Zou, Laser welding of ta15 titanium alloy and INCONEL 718 dissimilar metals. Archives of Metallurgy and Materials **67**, 1267-1276 (2022). DOI: https://doi.org/10.24425/amm.2022.141051

[2] N. Zong, W. Sun, X. Liang, T. Jing, Analysis of tilted columnar dendrites at grain boundaries during wire and laser additive manufacturing: A phase-field study. Archives of Metallurgy and Materials **68**, 469-475 (2023). DOI: https://doi.org/10.24425/amm.2023.142424

[3] R. Kosturek, L. Sniezek, K. Grzelak, M. Wachowski, Research on the Microstructure of Laser Beam Welded Sc-Modified AA2519-F Extrusion, Archives of Metallurgy and Materials **67**, 773-778 (2022). DOI: https://doi.org/10.24425/amm.2022.137817

[4] Y.U. Jinling, Z. Zhentai, L.I. Shuai, D. Guo, L. Chang, EffEcts of Y2o3 on MicrostructurE and corrosion ProPErtiEs of LasEr cLadding coMPositE coatings on 304 stainLEss stEEL substratE. Archives of Metallurgy and Materials **68**, 447-453 (2023). DOI: https://doi.org/10.24425/amm.2023.142421

[5] M.N. Baba, G.D. Voinea, M.E. Lucaci, Three-Point Bending Response of Nylon 12 Obtained by Fused Filament Fabrication (FFF) Versus Selective Laser Sintering (SLS). Arch. Metall. Mater. **68**, 1439-1446 (2023). DOI: https://doi.org/10.24425/amm.2023.146210

[6] M. Jażdżewska, Effects of Co_2 and Nd:YAG Laser Remelting of the Ti6Al4V Alloy on the Surface Quality and Residual Stresses. Advances in Materials Science **20**, 82-90 (2020). DOI: https://doi.org/10.2478/adms-2020-0005

[7] S. Mohanty, M. Mukherjee, C. Mandal, S.M. Shariff, M. Aqeel, A. Senapati, T.K. Pal, Understanding the microstructural evolution and tensile characteristics of low nickel austenitic stainless-steel welds fabricated by diode LASER. International Journal of Pressure Vessels and Piping **206**, 105087 (2023). DOI: https://doi.org/10.1016/j.ijpvp.2023.105087

[8] X. Wang, Z. Zhang, Y. Zhao, Z. Hu, X. Li, Macroscopic morphology and properties of cobalt-based laser cladding layers on rail steel based on pulse shaping. Opt. Laser Technol. **168**, 109940 (2024). DOI: https://doi.org/10.1016/j.optlastec.2023.109940

[9] A. Dwivedi, M.K. Khurana, Y.G. Bala, R. Paraveen, Effect of heat treatment on microstructure and mechanical properties for laser powder bed fusion of nickel-based superalloy: A review. Mater. Today Proc. **115**, 280-288 (2023). DOI: https://doi.org/10.1016/j.matpr.2023.09.093

[10] A. Aminzadeh, J. Silva Rivera, P. Farhadipour, A. Ghazi Jerniti, N. Barka, A. El Ouafi, F. Mirakhorli, F. Nadeau, M.O. Gagné, Toward an intelligent aluminum laser welded blanks (ALWBs) factory based on industry 4.0; a critical review and novel smart model. Opt. Laser Technol. **167** (2023). DOI: https://doi.org/10.1016/j.optlastec.2023.109661

[11] P. Zhao, X. Zhang, S. Bian, W. Zhang, Z. Cao, Effect of preheating temperature on the defects in pulsed laser welding of sheet AZ31 magnesium alloy. Mater. Lett. **355** (2024). DOI: https://doi.org/10.1016/j.matlet.2023.135438

[12] K.Y. Benyounis, A.G. Olabi, M.S.J. Hashmi, Effect of laser welding parameters on the heat input and weld-bead profile. J. Mater. Process. Technol. **164-165**, 978-985 (2005). DOI: https://doi.org/10.1016/j.jmatprotec.2005.02.060

[13] J. Yin, G. Peng, C. Chen, J. Yang, H. Zhu, L. Ke, Z. Wang, D. Wang, M. Ma, G. Wang, X. Zeng, Thermal behavior and grain growth orientation during selective laser melting of Ti-6Al-4V alloy. J. Mater. Process. Technol. **260**, 57-65 (2018). DOI: https://doi.org/10.1016/j.jmatprotec.2018.04.035

[14] M. Ghayoor, S. Mirzababaei, K. Lee, Y. He, C. Chang, B. Paul, S. Pasebani, Strengthening of 304L stainless steel by addition of yttrium oxide and grain refinement during selective laser melting. In: Proceedings of the 30th Annual International Solid Freeform Fabrication Symposium – An Additive Manufacturing Conference, Austin, Texas, USA, 2019, pp. 967–976.

[15] B. AlMangour, M.-S. Baek, D. Grzesiak, K.-A. Lee, Strengthening of stainless steel by titanium carbide addition and grain refinement during selective laser melting. Materials Science and Engineering: A **712**, 812-818 (2018). DOI: https://doi.org/10.1016/j.msea.2017.11.126

[16] J.Z. Lu, K.Y. Luo, Y.K. Zhang, G.F. Sun, Y.Y. Gu, J.Z. Zhou, X.D. Ren, X.C. Zhang, L.F. Zhang, K.M. Chen, C.Y. Cui, Y.F. Jiang, A.X. Feng, L. Zhang, Grain refinement mechanism of multiple laser shock processing impacts on ANSI 304 stainless steel. Acta Mater. **58**, 5354-5362 (2010). DOI: https://doi.org/10.1016/j.actamat.2010.06.010

[17] J. Zhang, Y. Liu, M. Bayat, Q. Tan, Y. Yin, Z. Fan, S. Liu, J.H. Hattel, M. Dargusch, M.-X. Zhang, Achieving high ductility in a selectively laser melted commercial pure-titanium via in-situ grain refinement. Scr. Mater. **191**, 155-160 (2021). DOI: https://doi.org/10.1016/j.scriptamat.2020.09.023

[18] Z. Jiang, X. Chen, H. Li, Z. Lei, Y. Chen, S. Wu, Y. Wang, Grain refinement and laser energy distribution during laser oscillating welding of Invar alloy. Mater. Des. **186**, 108195 (2020). DOI: https://doi.org/10.1016/j.matdes.2019.108195

[19] D. Carluccio, M.J. Bermingham, Y. Zhang, D.H. StJohn, K. Yang, P.A. Rometsch, X. Wu, M.S. Dargusch, Grain refinement of laser remelted Al-7Si and 6061 aluminium alloys with Tibor® and scandium additions. J. Manuf. Process. **35**, 715-720 (2018). DOI: https://doi.org/10.1016/j.jmapro.2018.08.030

[20] D. Zhang, D. Qiu, S. Zhu, M. Dargusch, D. StJohn, M. Easton, Grain refinement in laser remelted Mg-3Nd-1Gd-0.5Zr alloy. Scr Mater. **183**, 12-16 (2020). DOI: https://doi.org/10.1016/j.scriptamat.2020.03.006

[21] J. Liu, M. Dahmen, V. Ventzke, N. Kashaev, R. Poprawe, The effect of heat treatment on crack control and grain refinement in laser beam welded β-solidifying TiAl-based alloy. Intermetallics (Barking) **40**, 65-70 (2013). DOI: https://doi.org/10.1016/j.intermet.2013.04.007

[22] Y. Wang, J. Shi, Y. Liu, Competitive grain growth and dendrite morphology evolution in selective laser melting of Inconel 718 superalloy. J. Cryst. Growth. **521**, 15-29 (2019). DOI: https://doi.org/10.1016/j.jcrysgro.2019.05.027

[23] K. Hattar, D.M. Follstaedt, J.A. Knapp, I.M. Robertson, Defect structures created during abnormal grain growth in pulsed-laser deposited nickel. Acta Mater. **56**, 794-801 (2008). DOI: https://doi.org/10.1016/j.actamat.2007.10.027

[24] A.I. Gorunov, O.A. Nyukhlaev, A.Kh. Gilmutdinov, Investigation of microstructure and properties of low-carbon steel during ultrasonic-assisted laser welding and cladding. The International Journal of Advanced Manufacturing Technology **99**, 2467–2479 (2018). DOI: https://doi.org/10.1007/s00170-018-2620-7

[25] Y. Chen, K. Zhang, J. Huang, S.R.E. Hosseini, Z. Li, Characterization of heat affected zone liquation cracking in laser additive manufacturing of Inconel 718. Mater. Des. **90**, 586-594 (2016). DOI: https://doi.org/10.1016/j.matdes.2015.10.155

[26] O.A. Idowu, O.A. Ojo, M.C. Chaturvedi, Effect of heat input on heat affected zone cracking in laser welded ATI Allvac 718Plus superalloy. Materials Science and Engineering: A **454-455**, 389-397 (2007). DOI: https://doi.org/10.1016/j.msea.2006.11.054

[27] E. Bayraktar, D. Kaplan, L. Devillers, J.P. Chevalier, Grain growth mechanism during the welding of interstitial free (IF) steels. J. Mater. Process. Technol. **189**, 114-125 (2007). DOI: https://doi.org/10.1016/j.jmatprotec.2007.01.012

[28] L.S. Derevyagina, A.I. Gordienko, A.M. Orishich, A.G. Malikov, N.S. Surikova, M.N. Volochaev, Microstructure of intercritical heat affected zone and toughness of microalloyed steel laser welds. Materials Science and Engineering: A. **770**, 138522 (2020). DOI: https://doi.org/10.1016/j.msea.2019.138522

[29] E. Biro, J.R. McDermid, J.D. Embury, Y. Zhou, Softening Kinetics in the Subcritical Heat-Affected Zone of Dual-Phase Steel Welds. Metallurgical and Materials Transactions A **41**, 2348-2356 (2010). DOI: https://doi.org/10.1007/s11661-010-0323-2

[30] X.-N. Wang, C.-J. Chen, H.-S. Wang, S.-H. Zhang, M. Zhang, X. Luo, Microstructure formation and precipitation in laser welding of microalloyed C–Mn steel. J. Mater. Process. Technol. **226**, 106-114 (2015). DOI: https://doi.org/10.1016/j.jmatprotec.2015.07.010

[31] T. Nanda, V. Singh, G. Singh, M. Singh, B.R. Kumar, Processing routes, resulting microstructures, and strain rate dependent deformation behaviour of advanced high strength steels for automotive applications. Archives of Civil and Mechanical Engineering **21**,7 (2021). DOI: https://doi.org/10.1007/s43452-020-00149-4

[32] Y. Shi, S. Wang, P. Zhang, Research on properties of ductile iron/mild steel joints welded by laser. Opt. Laser Technol. **164** (2023). DOI: https://doi.org/10.1016/j.optlastec.2023.109477

[33] B.P.-H. Liu, T.-F. Chung, J.-R. Yang, J. Fu, C.-Y. Chen, S.-H. Wang, M.-C. Tsai, C.-Y. Huang, Microstructure Characterization of Massive Ferrite in Laser-Weldments of Interstitial-Free Steels. Metals (Basel). **10**, 898 (2020). DOI: https://doi.org/10.3390/met10070898

[34] C. Yuce, M. Tutar, F. Karpat, N. Yavuz, The Optimization of Process Parameters and Microstructural Characterization of Fiber Laser Welded Dissimilar HSLA and MART Steel Joints. Metals (Basel). **6**, 245 (2016). DOI: https://doi.org/10.3390/met6100245

[35] P.G. Riofrío, J.A.M. Ferreira, C.A. Capela, Imperfections and Modelling of the Weld Bead Profile of Laser Butt Joints in HSLA Steel Thin Plate. Metals (Basel). **11**, 151 (2021). DOI: https://doi.org/10.3390/met11010151

[36] A.B. Pereira, R.O. Santos, B.S. Carvalho, M.C. Butuc, G. Vincze, L.P. Moreira, The Evaluation of Laser Weldability of the Third-Generation Advanced High Strength Steel. Metals (Basel) **9**, 1051 (2019). DOI: https://doi.org/10.3390/met9101051

[37] P. Švec, A. Schrek, T. Csicsó, Fiber Laser Welding of Dual-Phase and Bake-Hardened Steels. Strength of Materials **48**, 481-486 (2016). DOI: https://doi.org/10.1007/s11223-016-9789-5

[38] F. Matsui, M. Shibao, N. Yoshida, K. Shibata, H. Sakamoto, H. Sakurai, A. Hirose, K.F. Kobayashi, Property of Laser Welded Bake-Hardening Steel in Tailored Blanks for Automobile. Materials Science Forum **449-452**, 397-400 (2004). DOI: https://doi.org/10.4028/www.scientific.net/MSF.449-452.397

[39] H. He, F. Forouzan, J. Volpp, S.M. Robertson, E. Vuorinen, Microstructure and Mechanical Properties of Laser-Welded DP Steels Used in the Automotive Industry. Materials **45**, 614 (2021). DOI: https://doi.org/10.3390/ma14020456.

[40] E. Öztürk, H. Arıkan, Investigation of mechanical properties of laser welded dual-phase steels at macro and micro levels. Opt. Laser Technol. **157** (2023). DOI: https://doi.org/10.1016/j.optlastec.2022.108713

[41] M.S. Khan, M. Soleimani, A.R.H. Midawi, I. Aderibigbe, Y.N. Zhou, E. Biro, A review on heat affected zone softening of dual-phase steels during laser welding. J. Manuf. Process **102**, 663-684 (2023).
DOI: https://doi.org/10.1016/j.jmapro.2023.07.059

[42] A. Hamada, A. Khosravifard, S. Ghosh, M. Jaskari, M. Kreins, W. Abd-Elaziem, M. Wahba, E. Ahmed, T. Allam, Enhancement of strength in laser-joined Al-TRIP and Si-TRIP steels: Microstructural insights and deformation analysis. Materials Science and Engineering: A. **885** (2023).
DOI: https://doi.org/10.1016/j.msea.2023.145591

[43] M. Morawiec, M. Różański, A. Grajcar, S. Stano, Effect of dual beam laser welding on microstructure–property relationships of hot-rolled complex phase steel sheets. Archives of Civil and Mechanical Engineering **17**, 145-153 (2017).
DOI: https://doi.org/10.1016/j.acme.2016.09.007

[44] N. Contuzzi, M.E. Palmieri, A. Angelastro, Study on properties and microstructure of laser beam butt welded joints of Al-Si coated USIBOR® 1500 steel. Manuf. Lett. **33**, 38-41 (2022).
DOI: https://doi.org/10.1016/j.mfglet.2022.07.008

[45] M. Landowski, A. Świerczyńska, G. Rogalski, D. Fydrych, Autogenous Fiber Laser Welding of 316L Austenitic and 2304 Lean Duplex Stainless Steels. Materials **13**, 2930 (2020).
DOI: https://doi.org/10.3390/ma13132930

[46] J. Rojek, M. Hyrcza-Michalska, A. Bokota, W. Piekarska, Determination of mechanical properties of the weld zone in tailor-welded blanks. Archives of Civil and Mechanical Engineering **12**, 156-162 (2012). DOI: https://doi.org/10.1016/j.acme.2012.04.004

[47] M. Merklein, M. Johannes, M. Lechner, A. Kuppert, A review on tailored blanks – Production, applications and evaluation. J. Mater. Process. Technol. **214**, 151-164 (2014).
DOI: https://doi.org/10.1016/j.jmatprotec.2013.08.015

[48] ASTM E112 - 13. Standard Test Methods for Determining Average Grain Size, West Conshohocken, PA, USA (2013).
DOI: https://doi.org/10.1520/E0112-13

[49] EN 10130. Cold rolled low carbon steel flat products for cold forming – Technical delivery conditions (2006).

[50] G. Loporcaro, S. Pampanin, M.V. Kral, Long-term strain-ageing effects on low-carbon steel reinforcement. Constr Build Mater. **228**, 116606 (2019).
DOI: https://doi.org/10.1016/j.conbuildmat.2019.07.332

[51] ISO 13919-1. Electron and laser-beam welded joints – Requirements and recommendations on quality levels for imperfections – Part 1: Steel, nickel, titanium and their alloys. (2019).

[52] J. Nowacki, A. Sajek, P. Matkowski, The influence of welding heat input on the microstructure of joints of S1100QL steel in one-pass welding. Archives of Civil and Mechanical Engineering **16**, 777-783 (2016).
DOI: https://doi.org/10.1016/j.acme.2016.05.001

[53] L. Mei, D. Yan, J. Yi, G. Chen, X. Ge, Comparative analysis on overlap welding properties of fiber laser and CO2 laser for body-in-white sheets. Mater. Des. **49**, 905-912 (2013).
DOI: https://doi.org/10.1016/j.matdes.2013.02.003

[54] E. Zdravecká, J. Slota, Mechanical and Microstructural Investigations of the Laser Welding of Different Zinc-Coated Steels. Metals (Basel) **9**, 91 (2019).
DOI: https://doi.org/10.3390/met9010091

[55] H. Danielewski, A. Skrzypczyk, Steel Sheets Laser Lap Joint Welding – Process Analysis. Materials **13**, 2258 (2020).
DOI: https://doi.org/10.3390/ma13102258

[56] A. Lisiecki, R. Burdzik, G. Siwiec, Ł. Konieczny, J. Warczek, P. Folęga, B. Oleksiak, Disk Laser Welding of Car Body Zinc Coated Steel Sheets / Spawanie Laserem Dyskowym Blach Ze Stali Karoseryjnej Ocynkowanej. Archives of Metallurgy and Materials **60**, 2913-2922 (2015).
DOI: https://doi.org/10.1515/amm-2015-0465

[57] U. Prijanovič, M. Prijanovič Tonkovič, U. Trdan, M. Pleterski, M. Jezeršek, D. Klobčar, Remote Fibre Laser Welding of Advanced High Strength Martensitic Steel. Metals (Basel) **10**, 533 (2020). DOI: https://doi.org/10.3390/met10040533

[58] K.A.M.B. Gonçalves, G.L. de Faria, R.H.M. de Siqueira, T.R. de Oliveira, M.S.F. de Lima, Heat treatment effects on the hardness and wear behavior of laser-welded AISI40 martensitic steel plates. The International Journal of Advanced Manufacturing Technology **114**, 1155-1163 (2021).
DOI: https://doi.org/10.1007/s00170-021-06942-6

[59] J. Luo, J.J. Gao, H.X. Lin, Y.H. Fan, Y. Ran, H. Yin, H.B. Geng, Microstructure and tensile properties of the different thickness ASSAPH440 high strength steel/DC52D+ZF45 galvanized cold rolled sheet dissimilar metal welding joint by CO2 laser welding for automobile manufacturing. Mater Res Express **7**, 066513 (2020). DOI: https://doi.org/10.1088/2053-1591/ab99e9

[60] W.D. Antunes, M.S.F. de Lima, Experimental Development of Dual Phase Steel Laser-arc Hybrid Welding and its Comparison to Laser and Gas Metal Arc Welding. Soldagem & Inspeção **21**, 379-386 (2016).
DOI: https://doi.org/10.1590/0104-9224/SI2103.12

[61] M. Mihaliková, A. Lišková, M. Hagarová, J. Cervová, Fatigue Characteristics of Laser Welded DC06EK and DP600MC Steel Sheets. Acta Phys. Pol. A. **131**, 1347-1351 (2017).
DOI: https://doi.org/10.12693/APhysPolA.131.1347

[62] E. Bayraktar, D. Kaplan, C. Buirette, M. Grumbach, Application of impact tensile testing to welded thin sheets. J. Mater. Process. Technol. **145**, 27-39 (2004).
DOI: https://doi.org/10.1016/S0924-0136(03)00859-8

[63] M.S. Węglowski, K. Kwieciński, K. Krasnowski, R. Jachym, Characteristics of Nd:YAG Laser Welded Joints of Dual Phase Steel. Archives of Civil and Mechanical Engineering **9**, 85-97 (2009). DOI: https://doi.org/10.1016/S1644-9665(12)60072-7

[64] A. Kurc-Lisiecka, A. Lisiecki, Laser welding of the new grade of advanced high-strength steel Domex 960. Materiali in Tehnologije **51**, 199-204 (2017).
DOI: https://doi.org/10.17222/mit.2015.158

[65] T. Kik, Heat Source Models in Numerical Simulations of Laser Welding. Materials **13**, 2653 (2020).
DOI: https://doi.org/10.3390/ma13112653